



HAL
open science

Sources and distribution of fresh water around Cape Farewell in 2014

Marion Benetti, Gilles Reverdin, Jennifer S. Clarke, Eithne Tynan, Naomi Penny Holliday, S. Torres-Valdes, Pascale Lherminier, Igor Yashayaev

► **To cite this version:**

Marion Benetti, Gilles Reverdin, Jennifer S. Clarke, Eithne Tynan, Naomi Penny Holliday, et al.. Sources and distribution of fresh water around Cape Farewell in 2014. *Journal of Geophysical Research. Oceans*, 2019, 124 (12), pp.9404-9416. 10.1029/2019JC015080 . hal-02434907

HAL Id: hal-02434907

<https://hal.sorbonne-universite.fr/hal-02434907>

Submitted on 10 Jan 2020

HAL is a multi-disciplinary open access archive for the deposit and dissemination of scientific research documents, whether they are published or not. The documents may come from teaching and research institutions in France or abroad, or from public or private research centers.

L'archive ouverte pluridisciplinaire **HAL**, est destinée au dépôt et à la diffusion de documents scientifiques de niveau recherche, publiés ou non, émanant des établissements d'enseignement et de recherche français ou étrangers, des laboratoires publics ou privés.

Sources and distribution of fresh water around Cape Farewell in 2014

M. Benetti¹, G. Reverdin¹, J.S. Clarke^{2,3}, E. Tynan², N. P. Holliday⁴, S. Torres-Valdes^{4*}, P. Lherminier⁵, I. Yashayev⁶

¹Sorbonne Université, CNRS/IRD/MNHN (LOCEAN), 4 place Jussieu, F-75005 Paris, France.

² Ocean and Earth Sciences, University of Southampton, Waterfront Campus, National Oceanography Centre Southampton, Southampton, United Kingdom

³ Chemical Oceanography, GEOMAR Helmholtz-Zentrum für Ozeanforschung, Kiel, Germany

⁴National Oceanography Centre, Europa Way, Southampton, SO14 3ZH, U. K.

⁵Ifremer, Univ. Brest, CNRS, IRD, Laboratoire d'Océanographie Physique et Spatiale (LOPS), IUEM, F-29280, Plouzané, France

⁶Department of Fisheries and Oceans, Ocean Sciences Division, Bedford Institute of Oceanography, P.O. Box, 1006 Dartmouth, N.S., B2Y 4A2, Canada

* Present address: Alfred Wegener Institute, Am Handelshafen 12
27570 Bremerhaven

Corresponding author: Gilles Reverdin gilles.reverdin@locean-ipsl.upmc.fr

ORCID ID <https://orcid.org/0000-0002-5583-8236>

Submitted to JGR oceans 20/02/2019; revised version 14/06/2019

Key point 1: surveys in spring 2014 show a large variability in fresh water and its composition with often a small signal of brine formation at subsurface in the East Greenland Coastal Current (EGCC)

Key point 2: the EGCC is found close to the coast east of Cape Farewell is found further offshore, whereas it is found closer to the shelf break, west of Cape Farewell

Descriptive heading of key sections

Introduction

Data and Methods

Results: Spatial distribution of the FW fractions

Discussion

Conclusion

Supplementary Material

Abstract

We investigate the origin of freshwater on the shelves near Cape Farewell (south Greenland) using sections of three hydrographic cruises in May (HUD2014007) and June 2014 (JR302 and Geovide) 2014. We partition the freshwater between meteoric water sources and sea ice melt or brine formation using the $\delta^{18}\text{O}$ of sea water. The sections illustrate the presence of the East Greenland Coastal Current (EGCC) close to shore east of Cape Farewell. West of Cape Farewell, it partially joins the shelf break, with a weaker near-surface remnant of the EGCC observed on the shelf southwest and west of Cape Farewell. The EGCC traps the freshest waters close to Greenland, and carries a brine signature below 50m depth. The cruises illustrate a strong increase in meteoric water of the shelf upper layer (by more than a factor 2) between early May and late June, likely to result from East and South Greenland spring melt. There was also a contribution of sea ice melt near the surface but with large variability both spatially and also between the two June cruises. Furthermore, gradients in the freshwater distribution and its contributions are larger east of Cape Farewell than west of Cape Farewell, which is related to the East Greenland Coastal Current being more intense and closer to the coast east of Cape Farewell than west of it. Large temporal variability in the currents is found between different sections to the east and south-east of Cape Farewell, likely related to changes in wind conditions.

Plain language summary:

Three successive hydrographic cruises in the spring 2014 surveyed the water masses on the shelf near Cape Farewell in South Greenland. Using information from the isotopic composition of sea water as well as salinity, it is possible to partition contributions of fresh water input on the shelves (compared to the nearby open ocean) that result either from inputs from river, glacier or precipitation, or from the melt (or formation) of sea ice. This is related to the ocean currents that were observed or deduced from hydrography. These indicate fresh water trapped near the coast associated with the East Greenland Coastal Current, mostly on the south-east side, but also partially found at the surface on the western side. At subsurface, this current carried water enriched in brines (due to upstream sea ice formation). A large variability is observed over the 45 days spanned by the spring cruises both for the fresh water content and sources, than for the current structure.

1. Introduction

1 The East Greenland Current (EGC) and the East Greenland Coastal Current (EGCC) are major
2 export routes for cold and fresh waters from the Arctic Ocean into the North Atlantic sub-polar
3 gyre (NASPG, including the Nordic seas) (Hansen and Østerhus, 2000, Bacon et al., 2002,
4 Sutherland and Pickart, 2008, Stanford et al., 2011). Variable freshwater transports carried along
5 the Greenland shelf and slope (Dickson et al., 1988, Yashayaev et al., 2007) and along the Labrador
6 Current have been pointed as major sources for the observed changes in surface salinity in the
7 western NASPG (Belkin, 2004; Tesdal et al., 2018) and in the freshwater content of the NASPG
8 (Curry and Mauritzen, 2005). Episodes such as the Great Salinity Anomaly (Dickson et al., 1988)
9 have been attributed to changes in outflow from the Arctic and were probably caused by a
10 particularly large freshwater (and sea ice) flow through Fram Strait (Belkin et al., 1998) having
11 reached the NASPG south of Denmark Strait. Moreover, a recent large increase in meltwater
12 originating from the Greenland ice sheets and the Canadian Archipelago since 2000 (Shepherd et
13 al., 2012) is likely to contribute to increased freshwater input through the different shelf and slope
14 currents forming the NASPG. The induced changes in surface salinity, and thus in surface density,
15 can then affect deep water-mass formation (Lazier, 1973, Latif et al., 2006).

16

17 The EGC follows the East Greenland shelf break from Fram Strait to the southern tip of Greenland
18 at Cape Farewell, exchanging water with the Arctic and Nordic seas as well as with the Atlantic
19 waters in the Irminger basin (Sutherland and Pickart, 2008, Jeansson et al., 2008). It is driven by
20 both winds and thermohaline circulation (Holliday et al., 2007). Salinity and temperature decrease
21 towards the coast which, as well as bottom bathymetry, contribute to the formation of a current
22 vein on the shelf closer to the coast, the East Greenland Coastal Current (EGCC). The EGCC
23 consists primarily of Arctic-sourced waters carried via a bifurcation of the EGC south of Denmark
24 Strait (Sutherland and Pickart, 2008), with significant inputs from the Greenland ice sheet melt
25 water and runoff (Bacon et al., 2002). It is primarily driven by a combined wind and fresh-water
26 forcing (Bacon et al., 2014, Le Bras et al., 2018). At the southern tip of Greenland, near Cape
27 Farewell, the EGCC either merges with the EGC to form the West Greenland Current (Holliday et
28 al., 2007), or it separates from the coast to get closer to the shelf break (Lin et al., 2018).

29

30 Exports of freshwater from the Greenland shelf and slope to the open ocean occur at different
31 locations. North of Denmark Strait (DS), a significant part of the liquid freshwater and sea ice

32 content of the EGC drifts into the Nordic Seas (Dickson et al., 2007; Dodd et al., 2009; de Steur
33 et al., 2015). South of DS, the dominant North-Easterly winds push the fresh water towards the
34 coast, limiting direct exchange with the Irminger Sea. However, denser shelf and slope waters in
35 the East Greenland spill jet, containing a small proportion of this freshwater, probably cascade into
36 the deep boundary Current (Pickart et al., 2005). At Cape Farewell, a branch of the EGC retroflects
37 towards the south to feed the Irminger Sea (Holliday et al., 2007), while the other part follows the
38 shelf towards the north forming the WGC, spilling partially into the Labrador Sea (Lin et al., 2018).
39 Around 61-62°N, drifters, as well as current fields estimated from altimetric sea level data show
40 that a large part of the fresh water carried by the WGC is transported into the interior Labrador
41 Sea (Luo et al., 2016).

42
43 Assuming a unique saline water source (Atlantic water, possibly modified by Pacific-derived
44 water), one can partition the remaining liquid freshwater in the EGC/EGCC system into i. meteoric
45 water (MW) which includes Arctic runoff, local and Arctic precipitation, as well as continental
46 glacial and snow melt from Greenland, and ii. a contribution of sea ice melt and formation (SIM;
47 as a fraction, this is positive when melt occurs and negative when brines are released as sea ice
48 forms). At Cape Farewell, studies showed that the proportion of Pacific Water (PW) having
49 entered from Bering Strait is usually weak compared to what is estimated from nutrient
50 measurements further North (Sutherland et al., 2009, de Steur et al., 2015, Benetti et al., 2017).
51 Thus, the saline water source in the region can be safely assumed to be mostly of Atlantic water
52 (AW) origin. The distributions of MW and SIM onto the Greenland shelf and slope are driven
53 largely by both seasonal and local variability in continental glacial and snow melt, sea ice presence
54 as well as water mass changes happening further north (e.g. Arctic runoff, sea ice processes). The
55 bathymetry of the shelf (Lin et al., 2018) and the exchanges with the fjords or along canyons also
56 play a role in the spatio-temporal distribution of the freshwater content. Earlier cruises near Cape
57 Farewell (Cox et al., 2010) suggested that the freshwater composition near Cape Farewell
58 experiences large interannual or decadal changes, with increased SIM contribution in 2004-2005
59 possibly related to large sea ice export at Fram Strait. The cruises used in these earlier studies all
60 took place in late summer/early autumn. Possible seasonal modulation was not explored.

61

62 This paper aims to identify the freshwater composition on the shelf and slope near Cape Farewell
63 on a subset of transects from May-June 2014 where samples were collected in the top 200 m for
64 oxygen 18 isotope ($\delta^{18}\text{O}$) and total alkalinity measurements. Using mass balance calculations
65 based on {salinity- $\delta^{18}\text{O}$ } pairs, we estimate MW and SIM fractions of the liquid freshwater. Then,
66 we discuss the spatial distribution of MW and SIM on the Greenland shelf and slope in order to
67 establish the pathways of freshwater around Cape Farewell. We also investigate the near-surface
68 changes over the short period separating the different transects (from mid-May to late-June), and
69 discuss what this implies on the variability of the different sources and pathways. In an appendix,
70 we discuss the possible use of total alkalinity data as a complementary tracer of SIM and MW
71 inputs.

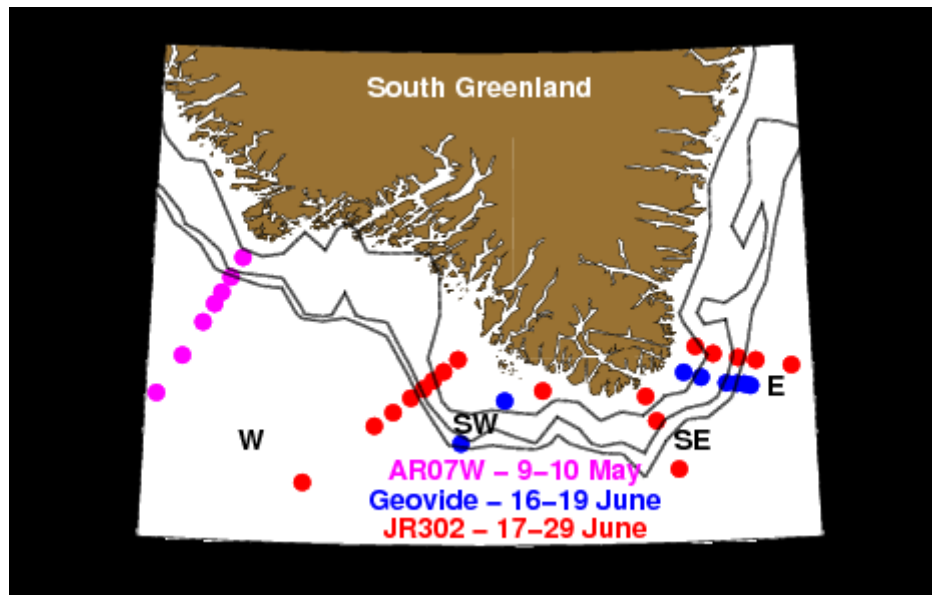
72 73 2. Data and methods

74 75 2.1. Cruises

76
77 We use data derived from three cruises sampling the Greenland shelf and slope around Cape
78 Farewell from mid May to late June 2014 (Figure 1). The first cruise (HUD2014007 AR07W)
79 crossed the southwestern Greenland shelf and slope ($\sim 60.5^\circ\text{N}$, 48°W) in mid-May on R/V Hudson
80 (Yashayaev et al., 2015). The second cruise Geovide (Sarhou and Lherminier, 2014) sampled the
81 east side of Greenland, reaching 20 km from the coast, in mid June (16-17 June). Furthermore, two
82 vertical profiles are available from the stations located on the south-west side of the Cape (18-19
83 June). The third cruise, JR302 (JR20140531) was conducted aboard the RRS James Clark Ross
84 (King and Holliday, 2015) on 17-29 June on the Greenland shelf and slope between 42 and 46°W ,
85 as a part of the OSNAP (Overturning in the Sub-polar North Atlantic Program) and RAGNARoCC
86 (Radiatively Active Gases from the North Atlantic Region and Climate Change) programs. Here,
87 we include three sections from this cruise, as well as one vertical profile on the inner shelf from
88 the station located at 44.67°N , 59.81°W , in front of a fjord. The easternmost section is very close
89 to the Geovide eastern section (a little to its north). Most sections were conducted during situations
90 of northeasterly to easterly (for E) and weak winds (western sections). The exception is section SE
91 of JR302 which was conducted during an episode of strong southwesterly wind, in particular close
92 to Greenland.

93 Salinity, temperature, oxygen 18 isotopic composition of H₂O ($\delta^{18}\text{O}$) have been measured for each
94 of these stations over the top 200 m. The vertical resolution of $\delta^{18}\text{O}$ measurements is not the same
95 on the different sections. The sections have different horizontal resolution, often missing the close
96 proximity of shore and inner shelf due to sea ice, or just lack of sampling.

97
98



99
100 Figure 1: Station sampling of the Greenland shelf and slope around Cape Farewell in May-June
101 2014 with salinity, temperature and $\delta^{18}\text{O}$ data. The different sections are named E, SE, SW and W.
102 The 100-m, 300-m and 500-m isobaths are outlined (black contours).

103
104
105

2.2. Measurements

106 Vertical temperature (T) and salinity (S) profiles were measured with a SBE 911 plus CTD
107 mounted on a rosette sampler during hydrographic stations on all cruises. The instruments were
108 calibrated before and after each cruise. Additionally, measurements were calibrated with salinity
109 samples analyzed on salinometers referenced to standard sea water. The accuracy in S is 0.002,
110 the international GO-SHIP standard (www.go-ship.org) (we express S in the practical salinity scale
111 of 1978, pss-78, with no unit).

112

113 Current data from ship acoustic Doppler current profilers (S-ADCP) during the cruises (75 kHz
114 RDI ADCP during JR302; 38 kHz and 150 kHz RDI during Geovide). Geovide data were not
115 detided and averaged along track over 1 km. During JR302, the Lowered ADCP station data were
116 better quality than S-ADCP, and they were processed using the Lamont Doherty Earth Observatory
117 IX software v8 (www.ldeo.columbia.edu/~ant/LADCP) (Holliday et al. 2018). The barotropic
118 tides at the time of each LADCP cast were obtained from the Oregon State University Tidal
119 Prediction software (volkov.oce.orst.edu/tides/otps.html) and once de-tided, the u and v
120 components were rotated to provide the velocity normal to the section (JR302 S-ADCP data are
121 referred to once in the text, but were not detided and are not shown). Two repeats of the western
122 section during HUD2014007 were obtained, which are very similar, and were not detided.

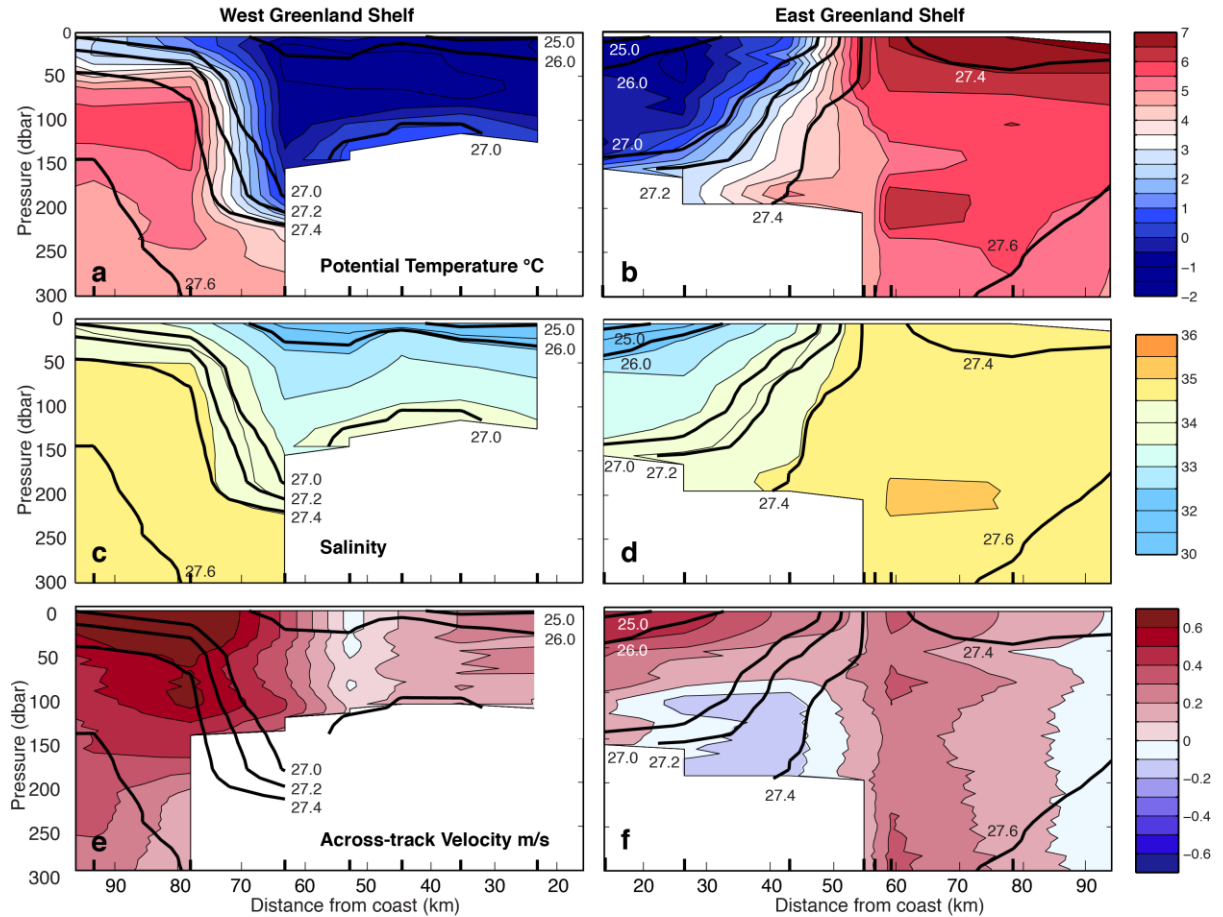
123
124 During the hydrographic stations, water samples were collected using a 24-bottle rosette equipped
125 with Niskin bottles. During JR302, water samples for $\delta^{18}\text{O}$ measurement were collected in 5 mL
126 screw top vials, sealed with parafilm and electrical tape. Samples were analysed at the NERC
127 isotope Geosciences Laboratory (NIGL) in East Kilbride after the cruise (Isoprime 100 with
128 Aquaprep; see Benetti et al (2017b) for instrumental set up). During the HUD2014007 and
129 Geovide cruises, water samples for $\delta^{18}\text{O}$ measurements were collected in 30 mL tinted glass bottles
130 (GRAVIS). The samples were analyzed with a PICARRO cavity ring-down spectrometer (CRDS
131 ; model L2130-I Isotopic H₂O) at LOCEAN (Paris, France). Based on repeated analyses of an
132 internal laboratory standard over several months, the reproducibility of the $\delta^{18}\text{O}$ measurements is
133 $\pm 0.05\%$. All seawater samples measured at LOCEAN have been distilled to avoid salt
134 accumulation in the vaporizer and its potential effect on the measurements [e.g., Skrzypek and
135 Ford, 2014]. Measurements are presented in the VSMOW scale, using reference waters previously
136 calibrated with IAEA references and stored in steel bottles with a slight overpressure of dry
137 nitrogen to avoid exchanges with ambient air humidity. Moreover, in order to fairly compare the
138 $\delta^{18}\text{O}$ measurements based on two different methods of spectroscopy (laser spectroscopy for
139 Geovide and Hudson cruise samples, mass spectrometry for JR302), we convert the measurements
140 in the concentration scale. We apply the correction of +0.14 ‰ defined by Benetti et al. (2017) for
141 the PICARRO measurements coupled with distillation (Hudson and Geovide cruises). As we are
142 not as certain of the salt effect for the IRMS used for JR302 data, we adjust the measurements on
143 the AW endmember at salinity 35 to the average value obtained for the other two cruises. This

144 adjustment is +0.10 ‰ (with a 0.02 uncertainty) and is close to the correction expected to convert
145 from the activity scale to the concentration scale, (Sofer et al., 1972, Benetti et al., 2017b; this
146 last paper also used NIGL measurements).

147
148 During the JR302 and Geovide cruises, total alkalinity samples were collected. We will use here
149 data from the JR302 cruise, which were measured according to Dickson et al. (2007). Water was
150 collected using silicone tubing into either 500 ml or 250 ml Schott Duran borosilicate glass bottles
151 and poisoned with saturated mercuric chloride solution (50 µL for 250 mL bottles and 100 µL for
152 500 mL bottles) after creating a 1 % (v/v) headspace. Samples were sealed shut with Apiezon L
153 grease and electrical tape and stored in the dark at 4 °C until analysis. JR302 TA samples were
154 analysed on board using two VINDTA 3C systems (Mintrop, 2004). Measurements were
155 calibrated using certified reference material (batches 135 and 136) obtained from Prof. A. G.
156 Dickson (Scripps Institute of Oceanography USA). The precision of the replicate and duplicate
157 measurements was 2.0 µmol.kg⁻¹ (King and Holliday, 2015).

158

159 2.3 T, S, current sections



160

161 Figure 2. Sections of potential temperature (a, b), salinity (c, d) and across-track velocity (LADCP)
 162 (e, f) from sections on the West Greenland Shelf (left column; June 17-18) and the East Greenland
 163 Shelf (right column; June 24-25) from JR302 sections W and E (Fig. 1). The distances are
 164 decreasing towards Greenland (between the two columns). Solid black lines are potential density
 165 contours, and the positive (red) currents corresponds to an anticyclonic current component around
 166 the tip of Greenland (southwestward for section E and northwestward for section W). The ticks
 167 along bottom axis indicate station positions.

168

169 The JR302 density (temperature and salinity) sections (Fig. 2) illustrate a strong tilted front on the
 170 shelf east of Cape Farewell, or near the shelf break for the section west of Cape Farewell,
 171 separating the cold and fresh waters of Arctic origin from the North Atlantic waters having
 172 circulated along the rim of the Irminger Sea in the East Greenland Current (EGC)/Irminger Current
 173 system. The slope of the isopycnals indicates that this front is baroclinic both east and west of

174 Greenland. This is also found in the current sections (e, f) where this front is associated with a
175 surface maximum of the current circulating anti-cyclonically around southern Greenland (Cape
176 Farewell). The baroclinicity is larger along section E (Fig. 2f), whereas the front is narrower and
177 more vertical (with less shear in the vertical) along section W (Fig. 2e). Along section W, there is
178 also a current closer to shore with little vertical shear, whereas the EGC is well defined and with
179 little vertical shear on section E, slightly offshore of the shelf break. The intensity of the different
180 flow components is different between these sections. Additionally, it was different for section E
181 with the Geovide section a week earlier presenting much larger currents on the shelf (by a factor
182 2). This is not surprising in this region where shelf currents are strongly sensitive to local (or
183 upstream) wind conditions (Le Bras et al., 2018), which presented large variability during the
184 period of the surveys (in particular, the Geovide E section happened following a period of large
185 northeasterly winds, whereas JR302 section E experienced strong northeasterly winds close to the
186 coast. We will loosely refer to the region on the shelf with a strong surface influence of Arctic
187 waters as the region of the EGCC, as it is usually associated with this current.

188

189 2.4 Mass balance calculation for Meteoric Water and Sea Ice Melt Fractions

190

191 We separate the mass contributions to the freshwater in SIM, MW, and AW inputs. We assume
192 that AW is the main saline sea water input to the system, since previous studies suggest the fraction
193 of PW around Cape Farewell is negligible (e.g. Sutherland et al., 2009), which differs from what
194 is sometimes observed upstream north of Denmark Strait in The EGC (de Steur et al, 2015). In
195 addition, we did not find that to be otherwise, as evidenced from AR07W section nutrient data
196 (Benetti et al., 2017). Benetti et al. (2016) calculated, in a similar hydrological context and in term
197 of freshwater inputs, that a variation of 20% in the PW fraction leads to a change of 1% on the
198 MW fraction and of 0.5 % on the SIM fractions. At Cape Farewell, from all available nutrient data,
199 we expect PW fractions lower than 5-10% (although winter and early spring data not affected by
200 biological production are rare). Thus, the error associated with neglecting PW is small compared
201 to the observed signals. To determine the fractions f_{SIM} , f_{MW} and f_{AW} , we follow the method of
202 Ostlund and Hut (1984) by solving end-member equations for mass, $\delta^{18}O$ and S (see eq. 1, 2 and
203 3).

204

205
$$f_{AW} + f_{SIM} + f_{MW} = 1$$

206 *Equation 1*

207
$$f_{AW} \cdot \delta^{18}O_{AW} + f_{SIM} \cdot \delta^{18}O_{SIM} + f_{MW} \cdot \delta^{18}O_{MW} = \delta^{18}O_m$$

208 *Equation 2*

209
$$f_{AW} \cdot S_{AW} + f_{SIM} \cdot S_{SIM} + f_{MW} \cdot S_{MW} = S_m$$

210 *Equation 3*

211 where subscript m denotes the measured value and with end-members values chosen with similar
212 values as in Benetti et al. (2016, 2017) (with $\delta^{18}O_{MW} = -18.4\%$, and $\delta^{18}O_{MW} = 0.50$).

213

214 Sensitivity tests were done in Benetti et al. (2016) to evaluate the impact of the uncertainties on
215 the calculation of f_{SIM} and f_{MW} in the Labrador Current, and we expect similar uncertainties for
216 these Cape Farewell sections. In short, there is little impact on the fraction calculations related to
217 the SIM properties, and more sensitivity to the end-member $\delta^{18}O_{MW}$. Most commonly, Benetti et
218 al. (2016) and other studies (such as Cox et al., 2010) have suggested uncertainties of 1–2%.

219 We applied the same mass balance equations but using TA instead of oxygen isotope data of the
220 JR302 cruise. The comparison between estimations of MW and SIM fractions by the two methods
221 is discussed in supplementary material. In short, the general trend of the FW distribution is similar
222 using the two methods, with correlation coefficients higher than 0.7. Nevertheless, MW and SIM
223 fraction calculations appear noisier using TA measurements, as they are affected by biological
224 activity as well as by exchanges with particles in shallow waters and coastal environments (Fry et
225 al., 2015), while $\delta^{18}O$ computation is not sensitive to biological processes. There is also a
226 variability in TA originating from polar water in the spring (Nondal et al., 2009), possibly
227 associated with exchanges with particles or sea ice that is not taken into account in the method.
228 This will affect MW and SIM fraction calculations. Furthermore, a common limitation to the two
229 methods results from the choice of the specified end-members. Indeed, TA and/or $\delta^{18}O$ of MW
230 sources widely vary as a function of the freshwater origins (local or remote inputs from Greenland
231 ice sheet, local spring snow melt or river runoff with an arctic origin).

232

233 3. Results: Spatial distribution of the FW fractions

234 We will present observations over the shelf, from sections starting upstream of Cape Farewell
235 along east Greenland, then south of Greenland (sections SE and SW), and ending with the
236 sections to the west of Cape Farewell. On all section plots, we will indicate isopycnals 25.5, 26.5
237 and 27.5 when they are intersected. A downward slope of the isopycnals towards the coast is
238 often found that is indicative of a surface intensification of the coastal current. The coast will be
239 on the left side of the plots for sections east of Cape Farewell, and on the right side, for sections
240 west of Cape Farewell.

241

242 3.1 East Greenland shelf

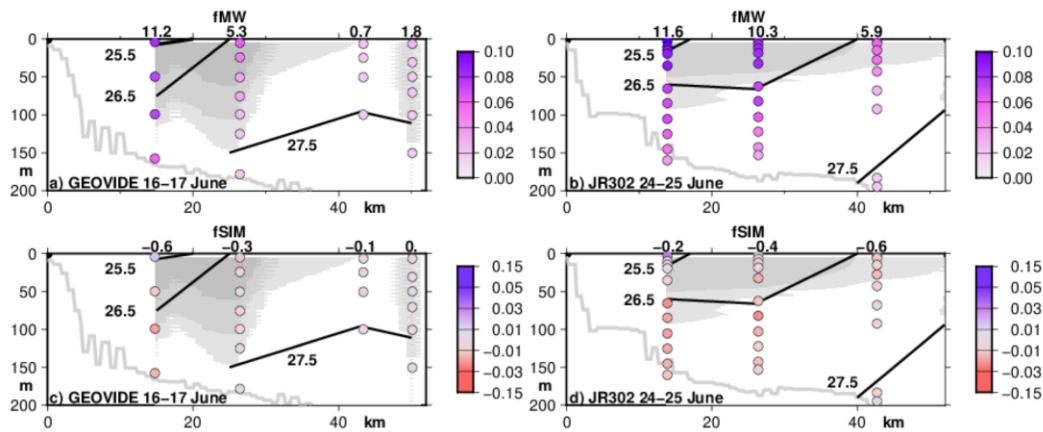
243

244 Figure 3 presents the SIM and MW fractions for the two eastern sections during Geovide (mid-
245 June, 16-17 June; left panels a, c) and JR302 (24-25 June; right panels b, d) (see location in Figure
246 1). The spatial distribution of f_{MW} presents a similar pattern for the two sections, with an increase
247 shoreward and to the surface where there is freshening. We notice significantly higher MW
248 fraction values on 24-25 June (maximum 0.11) (Fig. 1b) compared with the earlier 16-17 June
249 section (maximum 0.08) (Fig. 1a). Interestingly, during Geovide there was an additional CTD cast
250 done at 17 km, i.e. 1.5 km further from the coast than the plotted inshore station. It presents higher
251 salinity (often by 0.3) and warmer temperature, indicating large horizontal gradients. Thus, there
252 might be even lower salinity/temperature and larger MW fractions closer to the coast than at the
253 station at 15,5 km from the coast. So we suspect that the unsampled area inshore is rich in MW,
254 with values as large as the ones observed at the JR302 station 14 km from shore. For f_{SIM} (Fig.
255 3b,d), positive values are only observed on both sections very close to the surface and mostly at
256 the inner station. The stronger f_{SIM} are observed in late June during JR302 (surface maximum of
257 0.03 at the innermost station). On both sections, negative f_{SIM} values (-0.01/-0.02), indicating a
258 signal of brines, are observed near 100 m depth. Notice that the brine signal is not present at the
259 station ~52 km from the coast close to the shelf break, where f_{SIM} is close to 0. Furthermore, on
260 Geovide section (left panel), the brine signal is not found already 26 km from the coast. Thus, all
261 the negative f_{SIM} values as well as the large MW fractions are within the EGCC based on the
262 current data, whereas the outer stations on the shelf are outside the southward flow of the EGCC.

263

264 The differences between the two sections suggest an offshore shift of the structure between the
 265 Geovide and JR302 sections, as well as a diminution of the surface peak velocities. Although there
 266 is a difference in bathymetry between the two sections, it does not seem large enough to explain
 267 the shift, which is probably more the result of temporal evolution during the 8 days separating the
 268 two surveys, despite both sections being done in ice-free water.

269
 270
 271



272
 273 Figure 3: Spatial distribution along section E (left Geovide; right, JR302) of f_{MW} fractions (top a,
 274 b with water column inventories in m reported on top of each station) and f_{SIM} (bottom c, d with
 275 top 50-m inventories in m reported on top of each station). The x axis is the distance (km) to the
 276 coast (the coast is to the west). The Y axis is the depth (m). The light grey line indicates the bottom
 277 depth from ETOPO1. The isopycnal contours for 25.5, 26.5 and 27.5 kg/m^3 are also sketched, as
 278 well as the cross-track currents with grey shading for currents larger than 20 cm/s (darker greys
 279 for currents larger than 30 cm/s and 50 cm/s ; those currents are southward, and are not plotted west
 280 of the station closest to shore, where they were not measured).

281

282

283 3.2 South of Cape Farewell

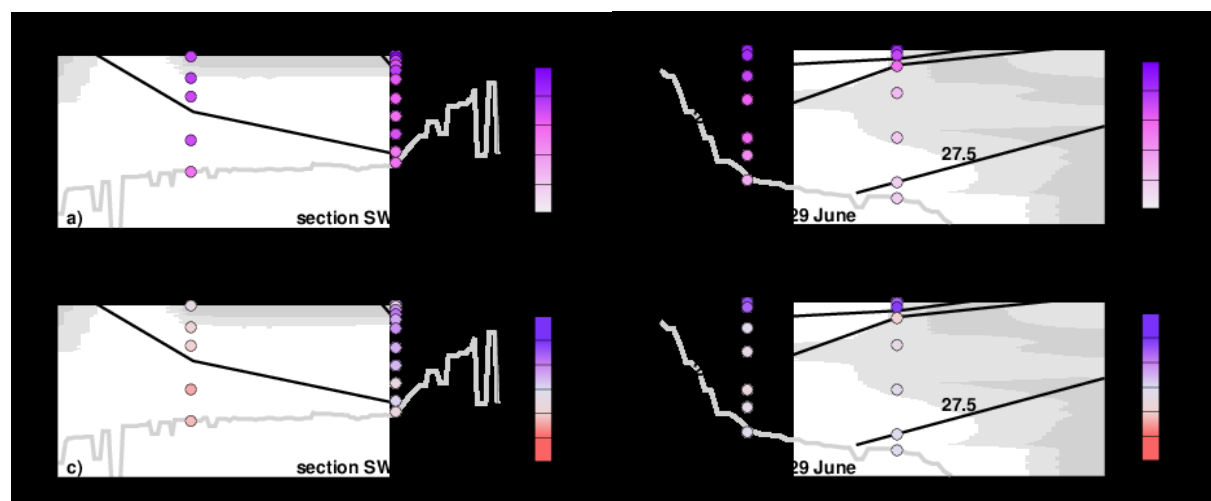
284

285 Figure 4 presents the fresh water distributions obtained from two sections located close to the
 286 southern tip of Cape Farewell, to its southwest and southeast. Similarly to what we have discussed

287 for the E sections, section SE (June 29) shows an increase shoreward and to the surface of MW
288 fractions with strong values of 0.07-0.08 at the surface on the two innermost stations. Near zero
289 MW fractions (Fig. 4b) are calculated at ~67 km from the coast (after the shelf break; not shown).
290 We calculated strong SIM inputs (fractions of 0.04-0.05) over the top 20 meters of the two inner
291 shelf stations, whereas subsurface samples show SIM fractions close to 0 (Fig. 4d). On the SADC
292 section taken just before the station 109 closest to shore, currents were weak and decreasing at
293 subsurface towards the shore, and with reversed currents at the surface and near bottom. This
294 section was taken during a short episode of strong southwesterly wind, which probably induced
295 this near-coastal current reversal. The strong baroclinicity is seen both in the isopycnal slope
296 towards the coast and the current profiles (not shown).

297
298 The left panels (Section SW) of Figure 4 (a,c) are based on stations located a bit further south-west
299 of Cape Farewell, and collected 8-11 days earlier than along section B. During the JR302 station
300 located in front of the fjord estuary (21 June), strong SIM inputs (0.02-0.03) are observed down to
301 80 m (Fig. 4c). MW are not particularly high at subsurface, whereas high MW fractions are only
302 found at the surface with a maximal value of 0.09 (Fig. 4a). The other station on the shelf, 36 km
303 from the coast, was sampled a little earlier on June 18 during Geovide. It shows strong MW inputs
304 ($f_{MW}=0.07$) down to 100 m and the presence of brines at subsurface ($f_{SIM}=-0.02$). This station
305 seems near the offshore edge of a weak coastal surface current, whereas the next station near the
306 shelf break with weak MW and SIM fractions (not plotted) is already within the EGC.

307
308



309

310 Figure 4: Same as Figure 3, but for the two most southern sections (coast to the right for section
311 SW and to the left for section SE). Section SW on the left to the south-west of Cape Farewell
312 combines the inshore station of JR302 (June 21) and GEOVIDE (June 18); section SE on the right
313 to the south-east of Cape Farewell is from JR302 (LADCP current at station closest to shore
314 replaced by SADCP currents taken just before arriving on station). Outer stations were cropped
315 from the plots, and present weak f_{MW} (except just at the surface) and f_{SIM} .

316

317

318 3.3 Southwest Greenland shelf

319

320 Figure 5 presents the fresh water distributions obtained from the two sections located on the west
321 side of Cape Farewell. The section HUD2014007 (AR07W) furthest to the west was sampled on
322 May 9, before the core of the melt season. Distinctively from the previously discussed late spring
323 sections, the MW and SIM distribution (Fig. 5a,c) are uniform for the two shelf stations with values
324 of 0.04-0.05 for MW and close to 0 for SIM. Potential density also presents little vertical or
325 horizontal gradients on the shelf, with weak northwesterly currents presenting a slight maximum
326 on the middle shelf.

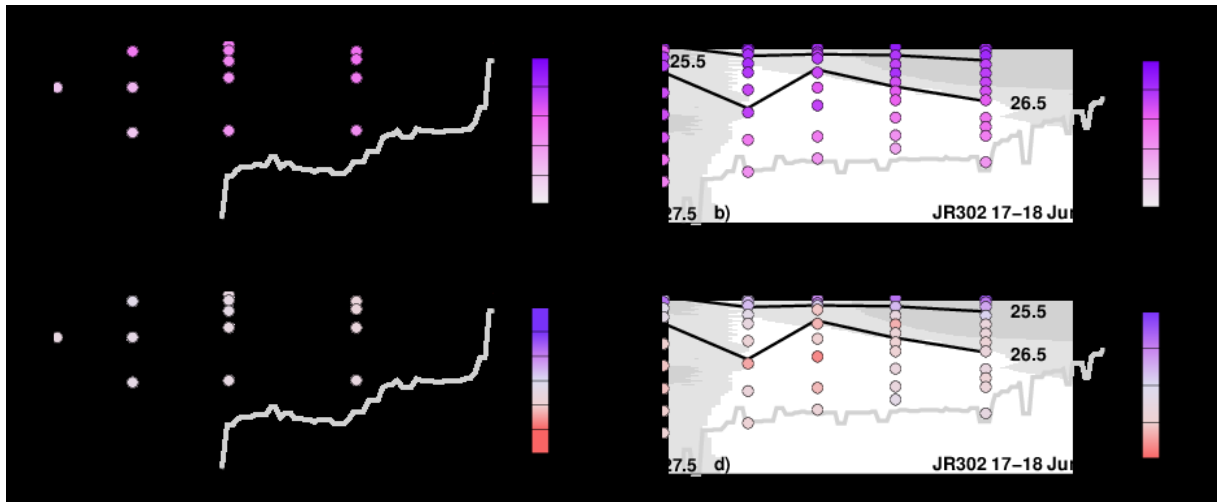
327

328 For the JR302 section (17-18 June) located further south (Fig. 5b, d), the MW contribution is close
329 to that observed during AR07W at depth, but increases toward the surface in the top 100 m.
330 Positive SIM fractions are observed near the surface (0-25 m) (Fig. 5d). For MW and SIM, the
331 freshwater extends across the full shelf, instead of being only found in the inner part as is observed
332 in the eastern sections discussed earlier. At subsurface, negative values of f_{SIM} (-0.01 to -0.02) are
333 found in the June section over the outer part of the shelf (at 44 and 52 km from the coast). Notice
334 that the brines influence has a similar magnitude to the one observed on section SW (Fig. 4c, 36
335 km from the coast). In both cases, they are also found outside of the branch of the northwestward
336 current closest to the coast.

337

338

339



341

342 Figure 5: Same as Figure 3, but for the western sections W (coast to the right). The May
 343 AR07W section is to the left (a,c), and the June JR302 section is to the right (b,d). No current
 344 velocity is plotted for AR07W.

345

346

347 4. Discussion

348

349 The AR07W cruise (May 9) gives a snapshot of the freshwater distribution on the SW Greenland
 350 shelf downstream of Cape Farewell in an ice-free sector before the onset of the 2014 melting
 351 season. At this time, the MW distribution appears rather homogeneous over the shelf, with
 352 integrated freshwater contents between 5.0-m (close to the coast) and 3.6-m (near shelf break).
 353 Moreover, SIM fraction values close to zero suggest a balance at this time between sea ice melt
 354 and sea ice formation (note that this result is sensitive to the choice of end-members). The profiles
 355 are only weakly stratified (0.3°C and 0.3 psu from top to bottom for the inner shelf station), which
 356 indicates that there was vertical mixing, as is typical of southwestern Greenland shelves in early
 357 spring.

358

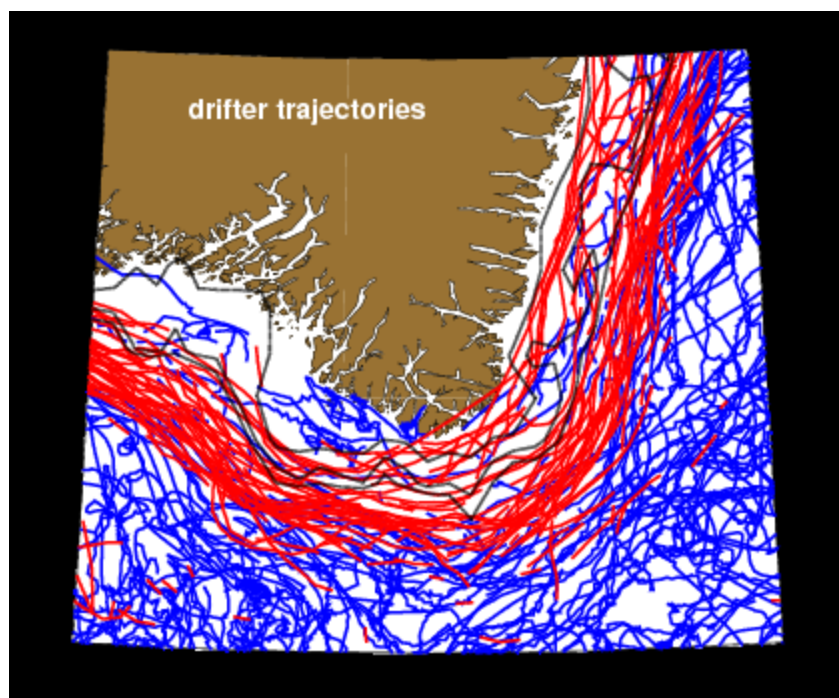
359 Then, in late spring 2014 from mid to late June, strong MW and SIM inputs are observed near the
 360 surface and on the shelf, with between 7 and 11.5-m total freshwater content on the southwestern
 361 shelf, but also close to the coast east of Cape Farewell. The two near-repeats of the eastern section
 362 E reveal that the freshwater variability can be strong at the synoptic time scale, with fast changes

363 in the freshwater distribution to the EGC/EGCC system (~8 days between the two realizations of
364 the section). A large part of the freshwater content increase in JR302 relative to earlier Geovide E
365 section could be explained by an outward displacement (by 15 km) or an increase in extent of the
366 core of the EGCC, both being compatible with the observed current sections. In addition, during
367 the later JR302 E section, there are also lower surface salinities (by at least 0.5), which could be
368 contributed by an increase in SIM in the top 10m, but also by an increase in MW. However,
369 because of the poor resolution of the large horizontal gradients, and also of the vertical gradients
370 for Geovide, it is not possible to be quantitative. Nonetheless, the changes in MW and SIM
371 (increase near the surface) are coincident with changes in the distribution of drifting sea ice
372 according to ice maps, suggesting the possible arrival of *storis* (multi-year ice) originating from
373 the Arctic which is known to penetrate in this region in May-July (Schmith and Hansen, 2003).
374 This might have been associated with the strong north-easterlies encountered during the JR302
375 repeat of the section on June 24-25. Remnants of 'old' sea ice were observed during some of the
376 JR302 sections, indicating that we are also missing the component of the freshwater contained in
377 the floating ice. However, with the very low partial coverage, this component probably remains a
378 very small contribution to the overall freshwater. Wind-related changes in EGCC current and
379 freshwater transport were also analyzed from a mooring array placed just afterwards (Le Bras et
380 al., 2018) with day to day transport changes almost by a factor of two. Large high frequency
381 changes of the freshwater transport on the shelf were also commented from mooring data north of
382 Denmark Strait (de Steur et al., 2017).

383
384 Most of the June 2014 sections suggest a subsurface signature of brines (near 100-m depth) at
385 some stations (f_{SIM} of -2%). Along the east side of Cape Farewell, the brine signal at subsurface is
386 close to the coast within the EGCC. It is further from the coast and closer to the shelf break for the
387 sections to the south-west (SW) and to the west of Cape Farewell. The brines are not found a week
388 later on the two stations of the JR302 section located south-east of Cape Farewell (section SE).
389 This might be either due the very low horizontal resolution of the section or due to synoptic
390 changes in the shelf water masses in less than 10 days. Synoptic changes in the water masses might
391 have resulted from wind having then veered to the southeast, coincident with the current section
392 showing the almost-disappearance of the EGCC on the inner shelf. Notice also that this brine signal
393 is much less than what is described further upstream during summer cruises north of Denmark

394 Strait (de Steur et al., 2015) indicating considerable changes in stratification and vertical mixing
395 between the two latitudes.

396
397 While the strong MW influence is found in the inner part of the eastern Greenland shelf in the
398 EGCC, the freshwater of MW or SIM origin is flowing towards the continental slope in the WGC
399 current, spreading near the surface over the full shelf, as well as over the continental slope. For the
400 southwest Greenland sections, this is near the shelf break that the largest freshwater inventories
401 are found, with values comparable to the ones on the inner shelf or the East Greenland sections.
402 This difference/change from the eastern side of Cape Farewell to its western side noticed here both
403 in near surface MW and SIM or in subsurface presence of brine-marked water is coherent with
404 observed separation of the EGCC core from the coast near Cape Farewell. See for example the
405 available 15-m drogued drifter trajectories (Global Drifter Program, Lumpkin et al., 2013), in
406 particular the ones with largest velocities (Figure 6). This is also observed in earlier summer cruises
407 (Holliday et al., 2007). This continuity of the freshwater content between the EGC and WGC has
408 already been observed in the study of earlier cruises (Cox, 2010) during the years 2005 and 2008.
409 This was also well described during one cruise with higher spatial resolution which took place
410 during the summer of 2014 (Lin et al., 2018), a few months after the surveys of this paper.



412 Figure 6. 15-m drogued drifter trajectories of the Global Drifter Program interpolated at a 6-hour
413 time step (AOML GDP GDAC site). The red color corresponds to velocities larger than 40 cm/s
414 (and blue color for lower velocities). The 100-m, 300-m and 500-m isobaths are outlined (black
415 contours).

416

417 In the set of sections used here, the resolution is often insufficient to discuss whether the EGCC
418 merges with the EGC or not on the southwestern sections. Indeed, the interruption of the
419 subsurface brine presence (negative SIM fractions) (Fig. 4d) in section SE south-east of Cape
420 Farewell suggests inadequate horizontal resolution, at least for that section. Interestingly, the
421 current sections both from GEOVIDE and JR302 suggest that a surface EGCC is still found near
422 the coast to the south-west and west of Cape Farewell, albeit with a much weaker amplitude than
423 to its east. Although this was not clearly identified during the May 2014 AR07W section, repeats
424 of the AR07W section in other years which ended closer to shore (such as in 2016) also found a
425 stronger surface EGCC close to shore. On the other hand, the presence of an EGCC on the
426 southwestern shelf in the 2014 spring surveys was not found in the late summer 2014 survey of
427 Lin et al. (2018). The large change of structure, stratification and meteoric water inventories
428 between May and June was surprising, even though the AR07W and JR302 are rather far apart.
429 However, an earlier occurrence of AR07W in June 1995 which also had water isotopic data
430 presents a structure much closer to the June 2014 JR302 section than to the May 2014 AR07W
431 section. This suggests that there might be a large seasonal change in the water masses on this part
432 of the shelf during this transitional season. The outward shift of the subsurface brine signal between
433 the eastern and the western June 2014 JR302 sections is also indicative, that at least below 50-m,
434 the EGCC joins the EGC closer to the shelf break between the two sections.

435

436 There is another anomaly that needs to be commented, which is that the JR302 station located in
437 front of the fjord system (near Narsarmijit) on section SW (Fig. 4a,c) shows an unusual deep
438 influence of SIM in the water column. The strong vertical mixing could be due to fjord processes
439 in the presence of strong winds and tides, as this fjord system also connects with east Greenland
440 and includes many inlets, islands and sills. Notice that for this station MW inputs are not
441 particularly high, compared to the strong SIM values, suggesting that at this time and in the fjord
442 system, SIM contribution is important relative to the MW inputs. It is also possible that a local

443 contribution of meltwater in this fjord with a less negative $\delta^{18}\text{O}$ isotope value than what we use,
444 could be mistaken as excess positive SIM.

445
446 The supplementary material discusses whether another approach on partitioning freshwater using
447 total alkalinity data could be used to complement the study. At this point, and although there is a
448 promising correlation between estimates of the two approaches, the approach using alkalinity
449 seems to be under-constrained. This is possibly due to contributions from unconsidered biological
450 processes and of the interaction between elements in solid and in dissolved forms that modify total
451 alkalinity, as particles have been found to be in rather large quantity in the inner shelf station of
452 the Geovide cruise (Tonnard et al, 2018). Indeed, two JR302 stations with alkalinity (but no water
453 isotope) data also provide a very striking deviation from what is expected, that we attribute to
454 massive particle influx, possibly from melting sea ice. This could also be the signature of
455 particularly alkaline spring polar water, as has been observed in early spring further north on the
456 east Greenland shelf (Nondal et al., 2009). Interestingly, this water is not observed at other sections
457 from the JR302 cruise. Thus, for those other sections, it was either trapped closer to the shore than
458 the first station, or its presence in this region is highly intermittent. Furthermore, this was not found
459 near south-east Greenland in the GLODAP hydrographic station data base (Olsen et al. 2016), nor
460 in any of the 8 late spring OVIDE cruises (between 2002 and 2016; the 2014 cruise being the
461 Geovide cruise of this paper, Perez et al. (2018)).

462

463 5. Conclusion and perspectives

464 This study was aimed at investigating the origin of freshwater on the shelves near Cape Farewell
465 during the late spring 2014. This was done with a simple partitioning between meteoric water
466 sources and sea ice melt or brine formation. We benefited from a set of three cruises which
467 illustrate the time variability of freshwater input. We clearly see a strong increase in meteoric water
468 in the shelf upper layer (by nearly a factor 2 or 4.5 m) between the May to late June season spanned
469 by the three cruises that likely results from east Greenland melting. There was also a contribution
470 of sea ice melt near the surface but with large spatial variability, as well as temporal variability
471 between the two June cruises. Furthermore, gradients in the freshwater distribution are larger east
472 of Cape Farewell than west of Cape Farewell, which is related to the East Greenland Coastal

473 Current being more intense and closer to the coast east of Cape Farewell than west of it. Also, we
474 observed a weaker surface-intensified EGCC southwest and west of Cape Farewell on the shelf on
475 all sections.

476
477 We also found a subsurface brine signal which tracks the EGCC subsurface pathway. During these
478 mid to late June surveys, it is found close to the coast east of Cape Farewell, but closer to the shelf
479 break west of Cape Farewell. This brine signal is unlikely to be an artefact of our identification of
480 end-members. It probably acquires its signature upstream on the east Greenland shelf or further
481 north during the previous winter when winter ice forms over a mixed layer reaching 50 to 100m
482 thickness. On the other hand, part of the variability near the surface both in time and in space could
483 be related to different sources of meteoric water (snow melt versus glacier melt, or different
484 glaciers or in the Arctic). A quantitative investigation would require higher spatial resolution
485 during the cruises, in addition to characterizing the current variability and better identifying the
486 different sources. The EGCC, in particular, is a rather narrow structure (core of 10-20 km width)
487 with a complicated path in this region (Holliday et al., 2007; Lin et al., 2018), which was not
488 sufficiently resolved during these cruises. For example, a strong variability in T and S vertical
489 profiles has been observed between different casts of the Geovide station closest to Greenland
490 along section E, which are only 1-2 km apart. The differences between the two near-repeats of the
491 eastern section (Geovide and JR302) seem more large scale and could be either associated with a
492 shift of the EGCC core away from the coast or an increase in its extension, together with a decrease
493 of its surface intensity. We expect that the differences between these two near-repeats of section
494 E, or with section B a little further south are associated with the different wind conditions
495 encountered and the associated response of the near-coastal ocean, as suggested by mooring data
496 a little more than 10 km from the coast along section E (Le Bras et al., 2018). We speculate that
497 this mooring could miss a significant part of the freshwater transport during the later spring-early
498 summer season, due to the very fresh water and currents trapped sometimes very close to the coast
499 and the sea surface, which could not be measured by this mooring. Furthermore, although the
500 current were well measured on this mooring, there are more data gaps in the salinity records, and
501 complementary measurements should be sought to complement its valuable records.

502

503 The sensitivity of the results to the particular sampling during these cruises could be
504 investigated/examined using eddy-resolving simulations with well resolved source waters along
505 eastern and southeastern Greenland. We expect large seasonal freshwater variability in this region
506 (Bacon et al., 2014), as also observed from mooring data (Le Bras et al., 2018), and thus it is not
507 surprising that there are significant differences with other surveys and sections that took place later
508 in summer and early autumn (Sutherland et al., 2009, Cox et al., 2010). For example, the brine
509 signal that we observed in June 2014 at depth is only found once in these published surveys. In
510 late summer, there might also be less influence of local freshwater sources and drifting sea ice,
511 thus a more direct connection to higher latitudes, or at least more integrated and less local. Further
512 upstream, near Denmark Strait, there has been evidence for large recent interannual variability in
513 the freshwater composition (de Steur et al., 2015). How this signal can be detected downstream,
514 and isolated from the fast variability found, at least during the spring surveys of the present study,
515 needs to be further investigated.

516 **Acknowledgments**

517 The authors would like to thank Mark Stinchcombe, Hannah Donald and Carolyn Graves for
518 collecting the nutrient data used in this work. The authors are also indebted to the isotope lab and
519 the other institutions that made their data available for the work.

520 JC was funded under The Analytical Chemistry Trust Fund, funded by the Royal Society for
521 Chemistry and the UK Natural Environment Research Council (NE/I019638/1) and GEOMAR.
522 ET was funded by RAGNARROC. MB was funded by the University of Iceland with support by
523 the National Power Company of Iceland Landsvirkjun. The authors would also like to thank
524 Matthew Humphreys, Claudia Fry and Alex Griffiths for their help analysing and collecting the
525 samples.

526
527 The Geovide cruise research was funded by the French National Research Agency (ANR-13-
528 BS06-0014), the French National Center for Scientific Research (CNRS-LEFE-CYBER), and
529 Ifremer. A special thank is also due to the R/V “Pourquoi Pas?” crew and Captain G. Ferrand, to
530 Géraldine Sarthou for her help, and to Arni Sveinbjörnsdottir for her encouragements.

531

532 JR302 and authors NPH, ET, STV were funded by NERC projects UK OSNAP (NE/K010875/1),
533 RAGNARRoCC (NE/K002511/1) and the Extended Ellett Line (National Capability). We
534 gratefully acknowledge the Atlantic Zone Off-Shelf Monitoring Program (AZOMP) of Fisheries
535 and Oceans Canada (DFO) ([http://www.bio.gc.ca/science/monitoring-monitorage/azomp-
536 pmzao/azomp-pmzao-en.php](http://www.bio.gc.ca/science/monitoring-monitorage/azomp-pmzao/azomp-pmzao-en.php)), including its participants and crew of CCGS Hudson.

537

538 Most of the hydrographic data will be available on the CCHDO website (hydrography and
539 nutrients) in the near future. Geovide hydrographic and current data are available (Lherminier
540 and Sarthou, 2017). The isotopic data were submitted to the free Global Seawater Oxygen-18
541 Database. The SADC data of GEOVIDE are here:

542 Lherminier Pascale, Sarthou Geraldine (2017). The 2014 Greenland-Portugal GEOVIDE CTDO2
543 hydrographic and SADC data (GO-SHIP A25 and GEOTRACES GA01).

544 SEANOE. <https://doi.org/10.17882/52153>.

545 The Geovide bottle data are available on SEANOE (<https://doi.org/10.17882/54653>). An update
546 is done (summer 2019) to include additional variables including $\delta^{18}\text{O}$. All the $\delta^{18}\text{O}$ data have
547 been transferred to GISS to be archived in 'Global Seawater Oxygen-18 Database'
548 (<https://data.giss.nasa.gov/o18data/>) (Schmidt et al., 1999)

549 The JR302 CTD, bottle and ADCP data are available from BODC

550 (https://www.bodc.ac.uk/resources/inventories/cruise_inventory/report/15037/).

551 The bottle data for AR07W (HUD2014007) are at CCHDO.

552 **References**

553 Bacon, S., G. Reverdin, I. G. Rigor, & Snaith, H. M. (2002). "A freshwater jet on the east
554 Greenland shelf," *J. Geophys. Res.* 107(C7).

555

556 Bacon, S., Marshall, A., Holliday, N. P., Aksenov, Y., & Dye, S. R. (2014). Seasonal variability
557 of the East Greenland coastal current, *J. Geophys. Res.*, 119(6), 3967-3987.

558

559 Belkin, I. M., Levitus, S., Antonov, J., & Malmberg, S. A. (1998). "Great salinity anomalies" in
560 the North Atlantic, *Prog. in Oceanography*, 41(1), 1-68.

561

562 Belkin, I. M. (2004). Propagation of the "Great Salinity Anomaly" of the 1990s around the
563 northern North Atlantic, *Geophys. Res. Lett.*, 31(8).

564

565 Benetti, M., Reverdin, G., Pierre, C., Khatiwala, S., Tournadre, B., Olafsdottir, S., & Naamar, A.
566 (2016). Variability of sea ice melt and meteoric water input in the surface Labrador Current off
567 Newfoundland, *J. Geophys. Res.*, *121*(4), 2841-2855.

568

569 Benetti, M., Reverdin, G., Lique, C., Yashayaev, I., Holliday, N. P., Tynan, E., et al. (2017).
570 Composition of freshwater in the spring of 2014 on the southern Labrador shelf and slope, *J.*
571 *Geophys. Res.*, *122*(2), 1102-1121.

572

573 Benetti, M., Sveinbjörnsdóttir, A. E., Ólafsdóttir, R., Leng, M. J., Arrowsmith, C., Debondt, K., et
574 al. (2017). Inter-comparison of salt effect correction for $\delta^{18}\text{O}$ and $\delta^2\text{H}$ measurements in seawater
575 by CRDS and IRMS using the gas-H₂O equilibration method, *Marine Chemistry*, *194*, 114-123.

576

577 Cox, K. A. (2010). Stable Isotopes as Tracers for Freshwater Fluxes into the North
578 Atlantic. *University of Southampton, School of Ocean and Earth Science, Doctoral Thesis*, 178pp.

579

580 Cox, K. A., J. D. Staford, A. J McVicar, E. J. Rohling, K. J. Heywood, S. Bacon, M. Bolshaw, P.
581 A. Dodd, S. de la Rosa, & Wilkinson, D. (2010). Interannual variability of Arctic sea ice export
582 into the East Greenland Current, *J. Geophys. Res.*, *115*, C12603, doi:10.1029/2010JC006227.

583

584 Curry, R., & Mauritzen, C. (2005). Dilution of the northern North Atlantic Ocean in recent
585 decades, *Science*, *308*(5729), 1772-1774.

586

587 Dickson, R. R., Meincke, J., Malmberg, S. A., & Lee, A. J. (1988). The “great salinity anomaly”
588 in the northern North Atlantic 1968–1982, *Progress in Oceanography*, *20*(2), 103-151.

589

590 Dickson, R., Rudels, B., Dye, S., Karcher, M., Meincke, J., & Yashayaev, I. (2007). Current
591 estimates of freshwater flux through Arctic and subarctic seas, *Progress in Oceanography*, *73*(3-
592 4), 210-230.

593

594 Dodd, P. A., Heywood, K. J., Meredith, M. P., Naveira- Garabato, A. C., Marca, A. D., &
595 Falkner, K. K. (2009). Sources and fate of freshwater exported in the East Greenland Current,
596 *Geophys. Res. Lett.*, 36(19).
597

598 Friis, K., A. Körzinger, & Wallace, D.W.R. (2003). The salinity normalization of marine
599 inorganic carbon chemistry data, *Geophys. Res. Lett.* 30 (2), 1085, doi:10.1016/S0009-
600 2541(99)00033-9.
601

602 Fry, C. H., T. Tyrrell, M. P. Hain, N. R. Bates, & Achterberg, E. P. (2015), Analysis of global
603 surface ocean alkalinity to determine controlling processes *Marine Chem.*, 174, 46-57.
604

605 Jeansson, E., Jutterström, S., Rudels, B., Anderson, L. G., Olsson, K. A., Jones, E. P., et al. (2008).
606 Sources to the East Greenland Current and its contribution to the Denmark Strait Overflow, *Prog.*
607 *in Oceanography*, 78(1), 12-28.
608

609 Hansen, B., & Østerhus, S. (2000). "North Atlantic-Nordic Seas exchanges." *Prog. in*
610 *Oceanography*, 45, 109-208.
611

612 Holliday, N. P., A. Meyer, S. Bacon, S. G. Alderson, & de Cuevas, B. (2007). "Retroflexion of
613 part of the east Greenland current at Cape Farewell." *Geophys. Res. Lett.* 34(7).
614

615 Holliday, N. P.; Bacon, S.; Cunningham, S. A.; Gary, S. F.; Karstensen, J.; King, B. A.; Li, F., &
616 McDonagh, E. L. (2018). [Subpolar North Atlantic overturning and gyre-scale circulation in the](https://doi.org/10.1029/2018JC013841)
617 [summers of 2014 and 2016](https://doi.org/10.1029/2018JC013841). *Journal of Geophysical Research: Oceans*, 123 (7). 4538-
618 4559.<https://doi.org/10.1029/2018JC013841>
619

620 King, B. A., & Holliday, N. P. (2015). RRS James Clark Ross Cruise 302, 06 Jun - 21 Jul 2014,
621 The 2015 RAGNARRoC, OSNAP and Extended Ellett Line cruise report, National Oceanography
622 Centre Southampton: 76.
623

624 Latif, M., Böning, C., Willebrand, J., Biastoch, A., Dengg, J., Keenlyside, N., et al. (2006). Is the
625 thermohaline circulation changing?, *J. Clim.*, 19(18), 4631-4637.
626

627 Lazier, J. R. N. (1973). The renewal of Labrador Sea water, *Deep Sea Research and*
628 *Oceanographic Abstracts*, 20, 4, 341-353. Elsevier.
629

630 Lin, P., R.S. Pickart, D.J. Torres, & Pacini, A. (2018). Evolution of the freshwater coastal current
631 at the southern tip of Greenland. *J. Phys. Oceanogr.*, 48 2128-2140, DOI: 10.1175/JPO-D-18-
632 0035.1.
633

634 Lherminier P., Sarthou, G. (2017). The 2014 Greenland-Portugal GEOVIDE CTDO2
635 hydrographic and SADCP data (GO-SHIP A25 and GEOTRACES GA01). SEANOE.
636 <https://doi.org/10.17882/52153>
637

638 Lumpkin, R., S. A. Grodsky, L. Centurioni, M.-H. Rio, J. A. Carton, & Lee, D. (2013). Removing
639 spurious low-frequency variability in drifter velocities. *J. Atmos. Oceanic Technol.*, 30, 353-360,
640 DOI: 10.1175/JTECH-D-12-00139.1.

641 Luo, H, R.M. Castelao, A.K. Rennermalm, M. Tedesco, A. Bracco, P.L. Yager, & Mote, T. L.
642 (2016). Oceanic transport of surface meltwater from the southern Greenland ice sheet. *Nature*
643 *Geosci.*, 25 April 2016, doi:10.1038/NGE2708.

644 Nondal, G., R.G.J. Belerby, A. Olsen, T. Johannessen, & Olafsson, J. (2009). Optimal evaluation
645 of the surface ocean CO2 system in the northern North Atlantic using data from voluntary
646 observing ships, *Limnol. and Oceanogr.: Methods*, 7(1), 109–118, doi:10.4319/lom.2009.7.109,
647 2009.

648 Olsen, A., R. M. Key, S. van Heuven, S. K. Lauvset, A. Velo, X. Lin, et al. (2016). The Global
649 Ocean Data Analysis Project version 2 (GLODAPv2) - an internally consistent data product for
650 the world ocean. *Earth System Science Data*, 8, 297-323. [doi:10.5194/essd-8-297-2016](https://doi.org/10.5194/essd-8-297-2016). Östlund,

651 H. G., & Hut, G. (1984). Arctic Ocean water mass balance from isotope data, *J. Geophys. Res.*,
652 89(C4), 6373-6381.

653 Perez, F. F., M. Fontela, M. I. Garcia-IBanez, H. Mercier, A. Velo, P. Lherminier, et al. (2018).
654 Meridional overturning circulation conveys fast acidification of the deep Atlantic Ocean. *Nature*,
655 554, 515–518 (22 February 2018).

656

657 Pickart, R. S., Torres, D. J., & Fratantoni, P. S. (2005). The East Greenland spill jet, *J. Phys.*
658 *Oceanogr.*, 35(6), 1037-1053.

659 Reverdin, G., Niiler, P. P., & Valdimarsson, H. (2003). North Atlantic Ocean surface currents. *J.*
660 *Geophys. Res.*, 108(C1).

661

662 Reverdin, G. (2010). North Atlantic subpolar gyre surface variability (1895–2009), *J. Clim.*,
663 23(17), 4571-4584

664

665 Rossby, T., Reverdin, G., Chafik, L., & Søiland, H. (2017). A direct estimate of poleward volume,
666 heat, and freshwater fluxes at 59.5° N between Greenland and Scotland, *J. Geophys. Res.*, 122(7),
667 5870-5887.a

668

669 Sarthou G., & Lherminier, P. (2014). GEOVIDE cruise, RV Pourquoi pas ?,
670 <https://doi.org/10.17600/14000200>

671

672 Schmidt, G.A., G. R. Bigg, & E. J. Rohling, E. J. (1999). "Global Seawater Oxygen-18 Database
673 - v1.22" <https://data.giss.nasa.gov/o18data/>

674

675 Schmith, T., & Hansen, C. (2003). Fram Strait ice export during the nineteenth and twentieth
676 centuries reconstructed from a multiyear sea ice index from southwestern Greenland. *J. Clim.*,
677 16(16), 2782-2791.

678

679 Shepherd, A., Ivins, E. R., Geruo, A., Barletta, V. R., Bentley, M. J., Bettadpur, S., et al. (2012).
680 A reconciled estimate of ice-sheet mass balance, *Science*, 338(6111), 1183-1189.

681
682 Sofer, Z., & Gat, J. R. (1972). Activities and concentrations of oxygen-18 in concentrated aqueous
683 salt solutions: analytical and geophysical implications, *Earth and Planetary Science Lett.*, 15(3),
684 232-238.
685
686 De Steur, L., Pickart, R. S., Torres, D. J., & Valdimarsson, H. (2015). Recent changes in the
687 freshwater composition east of Greenland, *Geophys. Res. Lett.*, 42(7), 2326-2332.
688
689 Sutherland, D. A., & Pickart, R. S. (2008). "The East Greenland Coastal Current: Structure,
690 variability, and forcing." *Prog. in Oceanography* 78(1): 58-77.
691
692 Sutherland, D. A., Pickart, R. S., Peter Jones, E., Azetsu- Scott, K., Jane Eert, A., & Ólafsson, J.
693 (2009). Freshwater composition of the waters off southeast Greenland and their link to the Arctic
694 Ocean. *J. Geophys. Res.*, 114(C5).
695
696 Tesdal, J. E., Abernathey, R. P., Goes, J. I., Gordon, A. L., & Haine, T. W. (2018). Salinity trends
697 within the upper layers of the subpolar North Atlantic. *J. Clim.*, 31(7), 2675-2698.
698
699 Tonnard, M., H. Planquette, A. R. Bowie, P. van der Merwe, M. Gallinari, F. Desprez de
700 Gésincourt, et al. (2018). Dissolved iron in the North Atlantic Ocean and Labrador Sea along the
701 Geovide section (GEOTRACES section GA01). *Biogeosciences Discuss.*,
702 <https://doi.org/10.5194/bg-2018-147>
703
704 Yashayaev, I., van Aken, H. M., Holliday, N. P., & M. Bersch (2007). Transformation of the
705 Labrador Sea water in the subpolar North Atlantic. *Geophys. Res. Lett.*, 34(22).
706

